

MINERvA Status Report and Request for 12×10^{20} POT in Antineutrino Mode

The MINERvA Collaboration

November 10, 2017

Abstract

The MINERvA experiment was designed to measure neutrino and antineutrino interaction cross sections in the 1-20 GeV range on a variety of nuclei in both the Low Energy and Medium Energy NuMI beam configurations. Low Energy data-taking completed in 2013, and the collaboration has now published twenty papers with that dataset, with several more near completion. Data taking in the Medium Energy neutrino-mode beam completed early this year, and the collaboration is actively working towards many cross-section measurements using those data. The experiment is currently taking Medium Energy antineutrino-mode data, and has requested an accumulated exposure of 12×10^{20} protons on target (POT) in this configuration. Given recent accelerator and detector performance, we expect to achieve this exposure by the 2019 summer shutdown. This document discusses the physics impact of a 12×10^{20} POT antineutrino ME exposure, and reviews the status of MINERvA detector operations and data analysis.

1 Introduction

Neutrino oscillation experiments rely on detailed models to predict neutrino energy spectra in their detectors given various oscillation scenarios. Precise predictions of neutrino-nucleus interaction cross sections are critical ingredients in these models. Although accelerator-based oscillation experiments are generally equipped with capable near detectors, they must rely on external cross-section measurements for the *a priori* models that form the basis of fits to their near and far detector data. As oscillation experiments such as T2K and NOvA accumulate more statistics and systematics become more important, their need for precise external measurements grows.

The MINERvA detector was designed to provide such measurements, and the MINERvA collaboration has produced twenty cross-section publications so far using data accumulated in the neutrino and antineutrino Low Energy NuMI configurations. We recently completed collecting 12×10^{20} POT in the neutrino-mode configuration of the Medium Energy NuMI beam. The search for CP violation in neutrino oscillations relies on measurements of both neutrino and antineutrino oscillations. T2K and NOvA have large samples of neutrino data and will spend the next year accumulating antineutrino data, making MINERvA's antineutrino results as important as our neutrino results.

When a neutrino interacts with a nucleus, the type of interactions that are available are primarily a function of the energy transferred to that nucleus, which is necessarily lower than the incoming neutrino energy. That means that even though MINERvA has average neutrino energies that are larger than those of NOvA or T2K (as shown in Figure 1), these experiments can and do use MINERvA’s results because we access the same low momentum transfers that their far detectors see. For the same reason, MINERvA provides cross-section measurements relevant to DUNE that are not accessible to lower energy experiments such as T2K, NOvA, or MicroBooNE.

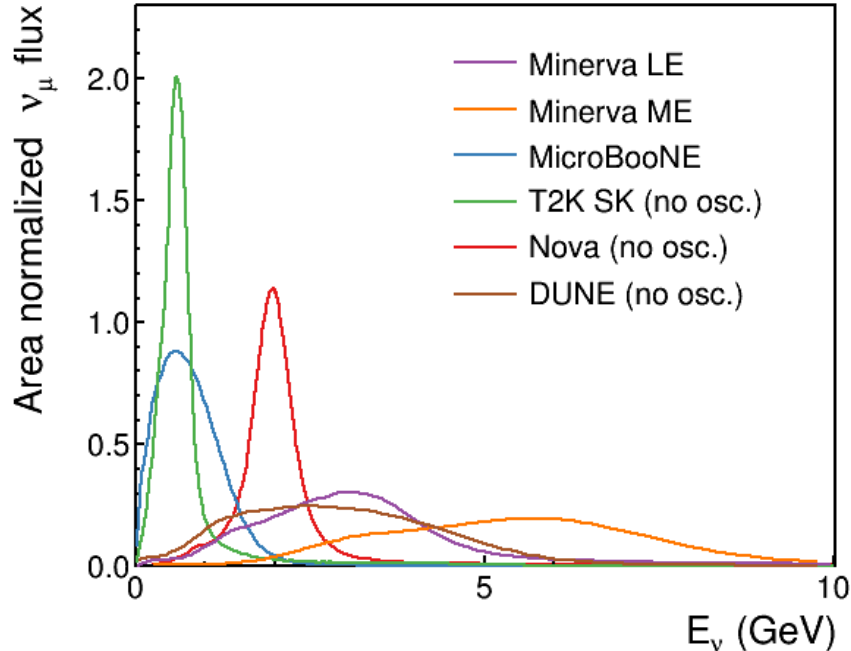


Figure 1: Neutrino fluxes normalized to the same area for the world’s accelerator-based oscillation experiments.

Since all modern neutrino experiments use targets made of heavy nuclei, event generators must include both models of primary neutrino interactions with nucleons and models of the nuclear medium in which the primary interaction occurs. Studies of cross sections on a single nucleus will necessarily measure the superposition of these two aspects of the interaction. However, measurements of the same process on different nuclei can separate the two effects. Because MINERvA includes targets composed of plastic scintillator (CH), carbon, iron, lead, water and helium, our measurements will test models of nuclear mass dependence, and in particular will inform models of nuclear effects in argon, which sits between carbon and iron on the periodic table.

MINERvA measurements are already benefiting the Fermilab oscillation program. For NOvA, MINERvA results and analysis procedures currently serve as sources of inspiration, guidance, and cross-checks for estimations of systematic uncertainties arising from cross sections that affect neutrino oscillation results. For example, the extent to which MINERvA

cross-section measurements for charged-current quasielastic scattering and neutrino pion production agree or deviate from GENIE¹ predictions provides guidance and checks for the final tune of NOvA’s reference simulation and for the error envelope that is assigned to it. The MINERvA neutrino flux prediction infrastructure is in use by MINOS+ and NOvA, and our neutrino flux measurements are guiding DUNE’s Near Detector design strategy.

MINERvA measurements have influenced all NOvA and most T2K ν_μ disappearance and ν_e appearance measurements to date, and will have similar influence as NOvA embarks upon oscillation measurements using antineutrinos. NOvA will look to MINERvA analyses of its antineutrino exposures for guidance as it undertakes construction of the error budget for its antineutrino oscillation measurements.

The MINERvA collaboration submitted a document describing our physics reach with 12×10^{20} protons on target (POT) in antineutrino mode to the Fermilab PAC in November 2014 [1]. This document presents preliminary results for several new analyses using a sample of antineutrino data already collected. These new analyses further support our request. We also provide a status report on neutrino-mode analyses in the Medium Energy beam and discuss the impact of our low energy data publications, detector performance, and operations cost.

2 Medium Energy Analyses

MINERvA took 3.4×10^{20} (2.0×10^{20}) POT in the NuMI beamline in the Low Energy neutrino (antineutrino) configuration between the years of 2009 and 2012. Starting in 2013 we began taking data in the Medium Energy configuration, and as of this writing we have recorded 12.0×10^{20} (3.7×10^{20}) POT in neutrino (antineutrino) running in that beam. Figure 2 shows the neutrino and antineutrino fluxes for the Low and Medium Energy beam tunes. The integrated neutrino flux per proton on target is a factor of 2.3 (2.1) larger in the Medium Energy beam than in the Low Energy beam in neutrino (antineutrino) mode. For processes whose cross section scales linearly with neutrino energy, the expected event rate is a factor of 3.4 (3.3) greater in the Medium Energy neutrino (antineutrino) beam.

The statistics and energy of the Medium Energy Beam mean that analyses that were only viable on the 6 ton scintillator target can now be done on the $\mathcal{O}(1)$ ton lead, iron, water, and graphite targets with comparable statistical precision to the Low Energy results. These publications will in turn provide better benchmarks for models that describe neutrino interactions on argon. In addition, the higher neutrino energies allow measurements to reach higher energy transfers and access new kinematic regions of the interactions that matter the most for oscillation experiments, especially DUNE.

2.1 Analysis Strategy

In the Medium Energy beam, not only is the neutrino flux per proton on target higher, but the number of POT per beam spill is higher, and the neutrino events themselves are more energetic than in the Low Energy beam. Figure 3 shows a typical event in the Medium

¹GENIE is a neutrino event generator used by many experiments, including NOvA, DUNE, and MINERvA

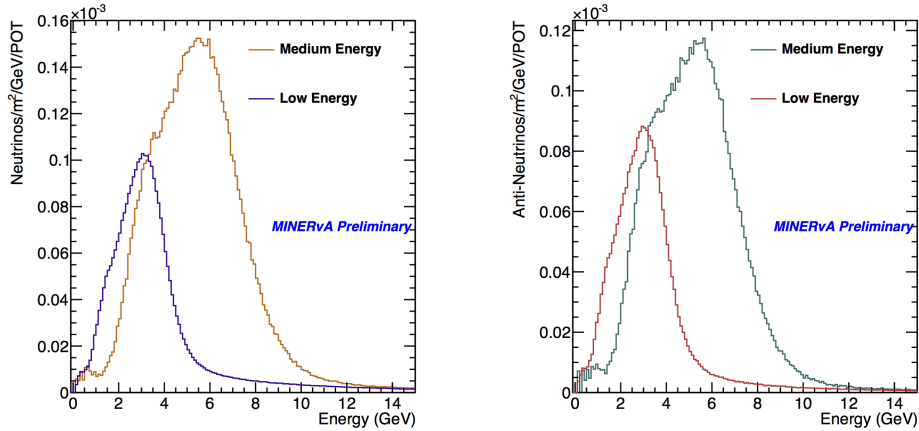


Figure 2: Neutrino (left) and antineutrino (right) fluxes per proton on target as a function of energy, for both the Low Energy and Medium Energy tunes of the NuMI beamline, as predicted by a GEANT4-based simulation.

Energy beam, a Deep Inelastic Scattering (DIS) event with activity in a large fraction of the detector. Because of all these factors, the intensity dependence of our event reconstruction is larger than in the Low Energy beam. In addition, the increase to 700 kW was accomplished incrementally, with several abrupt changes to the NuMI batch structure.

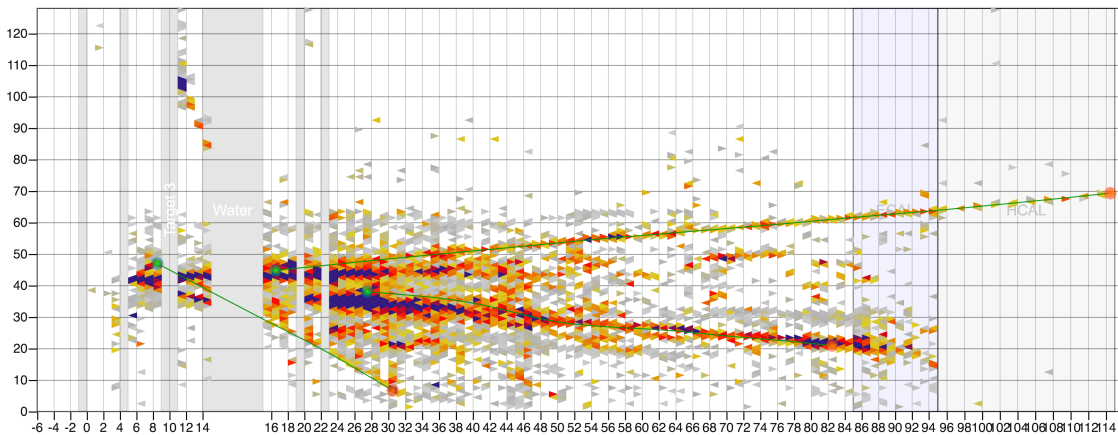


Figure 3: Simulated high occupancy event in MINERvA.

To address these changes, we have implemented many improvements to our simulation of accidental activity. In addition, a discrepancy between the predicted and measured neutrino flux using “standard candle” low recoil energy events indicates a likely problem with modeling of the NuMI Medium Energy focusing system. The collaboration has implemented a strategy to measure and correct this problem, described below.

MINERvA is also pursuing reconstruction improvements that will benefit all Medium Energy analyses. For example, we have changed the algorithm that uses timing information

to associate different groups of energy deposits with a specific neutrino interaction. We have also developed a machine learning algorithm that better identifies the vertex of events with large hadronic showers than our previous track-based algorithm. The event shown in Figure 3 is an example of a success of this algorithm. For this event, the track-based reconstruction correctly identified a muon exiting the back of the detector (right hand side), but failed to correctly find the vertex of the event. The Machine-Learning vertexing algorithm correctly placed the vertex in the second nuclear target from the front (left) of the detector.

MINERvA has chosen to implement all of these improvements while also developing analyses on a wide range of interaction channels. This means that there are currently several mature analyses of the Medium Energy data that are expected to be released within the next year.

2.2 Medium Energy Flux Prediction

In order to produce accurate cross-section measurements, MINERvA needs an accurate flux prediction, including both the absolute normalization and the shape as a function of neutrino energy. This section describes the two analyses that are addressing both of these aspects of the flux prediction and our plan to address an apparent mismodeling of the NuMI focusing system.

A measure of the total integrated energy-weighted flux comes from neutrino scatters on atomic electrons. MINERvA measured this process and constrained its flux in the low energy beam with about 100 events [2], and in the Medium Energy beam the higher event rate yields a larger sample size. The signature of neutrino-electron scattering is a single electron that is nearly parallel to the beamline axis. Figure 4 shows a distribution used to isolate this sample, the electron energy times the squared angle with respect to the beamline, for 9×10^{20} POT, and the electron energy distribution after all cuts. The statistical uncertainty on the total absolute flux will be well below 5%.

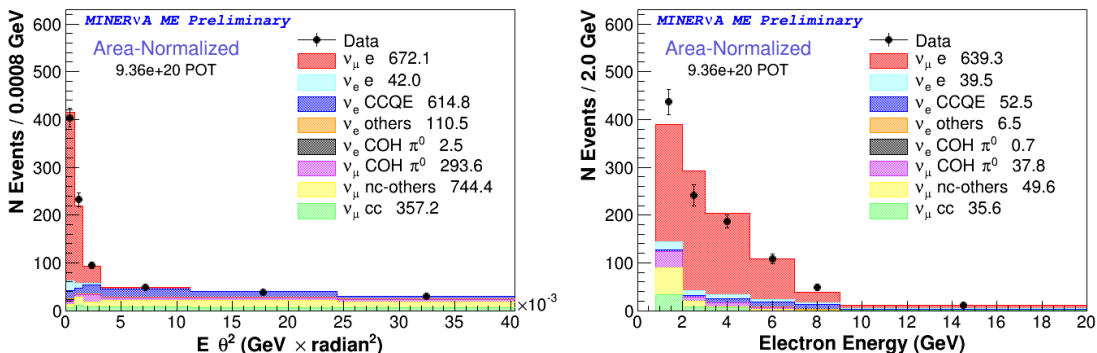


Figure 4: Left: the distribution of energy times the squared angle with respect to the beam for neutrino electron scattering candidates after all cuts but the one on this variable. Right: the electron energy distribution for the neutrino electron scattering candidates after all cuts.

A measure of the energy dependence of the neutrino flux comes from events that have low hadronic energy. These “low-nu” events have a known cross section with very little energy

dependence [3]. MINERvA has used this procedure in the past to measure its flux for a total inclusive cross section [4], but more generally it is used as a cross check of an *ab initio* flux prediction.

MINERvA has developed the state-of-the-art infrastructure for predicting the neutrino fluxes that come from 120 GeV protons striking a graphite target [5]. This infrastructure incorporates the world’s knowledge of hadron production and interaction measurements to normalize the hadron production predicted by GEANT4. This infrastructure has been adopted by NOvA, MINOS+, and DUNE for their flux predictions.

Even with this new infrastructure, the prediction for the peak of the NuMI on-axis flux in the Medium Energy beam appears to be shifted by a fraction of a GeV, as shown in Figure 5, which shows the event distribution in data and simulation for low-nu events. Since the energy dependence of this cross section is nearly zero, a discrepancy in the shape of this distribution suggests a flux problem rather than a cross-section problem. A similar discrepancy is seen in the antineutrino beam (left plot in Figure 9), and by MINOS+, and is not seen in a data set where the horns are turned off. This suggests that it is a focusing mismodeling rather than a hadron production mismodeling.

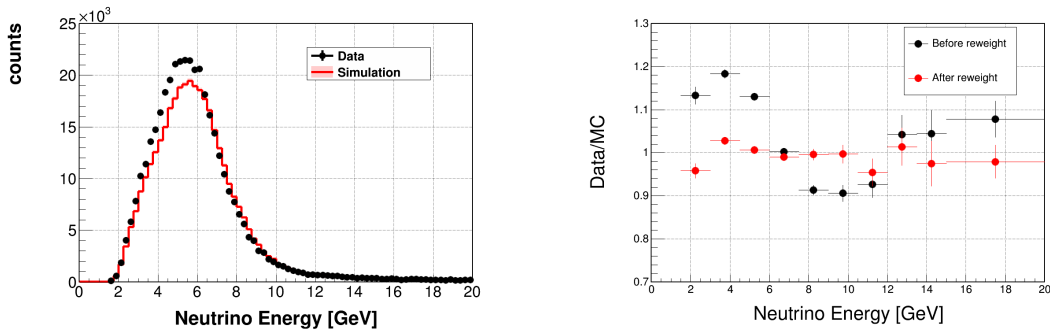


Figure 5: Left: The neutrino energy distribution for neutrino events with hadronic recoil less than 800 MeV, for both data and simulation. Right: the ratio of data to simulation before and after the focusing fit.

In order to produce a more accurate flux prediction, MINERvA has developed a strategy to fit the neutrino data-simulation discrepancy shown above for a number of possible focusing system effects: alignment, horn current, and primary beam parameters. The fit takes into account the fact that different alignment offsets will affect neutrino energy spectra differently in various transverse regions of the MINERvA detector. The data to simulation ratio before and after this fit is shown in the right of Figure 5. Because these focusing parameters affect the neutrino and antineutrino fluxes in the same way, the parameters that fix the neutrino discrepancy are also expected to correct the antineutrino discrepancy.

It should be noted that DUNE is planning to use both neutrino-electron scattering and the low-nu flux techniques that have been developed by MINERvA to achieve the required accuracy for their far detector flux prediction. Both of these analyses on MINERvA are helping to inform DUNE’s choices for its near detector complex.

2.3 Neutrino Analysis Progress

This section showcases the statistical power of a few of MINERvA’s Medium Energy neutrino analyses. The plots below do not incorporate our final flux prediction or final accidental activity simulation but do provide evidence that we are taking physics-quality data and have mature analyses that are progressing in parallel with the work described above.

Because the Medium Energy physics results will be focused on making comparisons between different nuclear targets, it is important to demonstrate that even in the intense Medium Energy environment the tracking and event reconstruction still works for exclusive final states like those with only two outgoing tracks. Figure 6 shows the vertex distribution for two-track events in three nuclear targets, and it is clear that the vertex resolution is adequate to isolate events on iron, lead, and carbon.

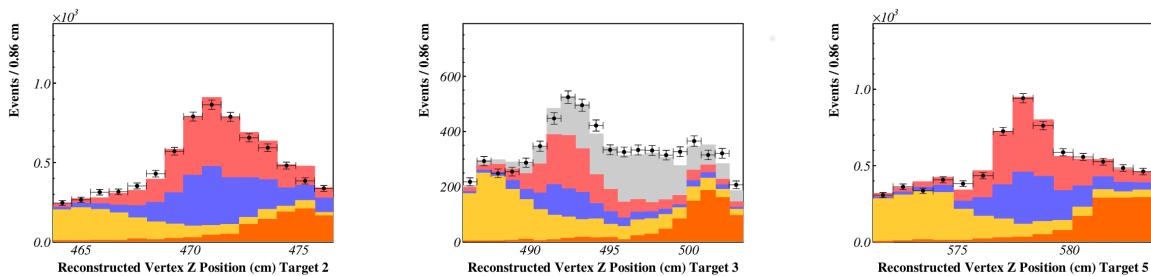


Figure 6: The vertex distribution along the detector’s longitudinal axis for events with two tracks in the region of three of our nuclear targets. Interactions originating in lead are in blue, iron in red, carbon in grey, and those coming from scintillator in yellow and orange.

Quasielastic scattering is a dominant channel in neutrino oscillation experiments given the energies of currently operating beams. In principle this is a two-body scattering process where for an incoming neutrino there is only an outgoing lepton and proton. However, the nucleus has an effect on both the initial and final state hadrons in this process. These effects change the outgoing particles and their kinematics, which in turn affect neutrino energy reconstruction. One measure of that nuclear effect is the angle between the neutrino-muon plane and neutrino-proton plane. Figure 7 shows this angle for the scintillator region, and two of our nuclear targets that are dominated by lead and iron, for a charged-current quasielastic analysis. Discrepancies in this distribution for higher atomic number are an indication that models of nuclear effects in quasielastic scattering need improvement.

Pion production is the next most copious channel for today’s oscillation experiments, and again MINERvA’s results will help guide the models of how the nucleus affects that process. Figure 8 shows the squared four-momentum transfer distribution for pion production candidates in the nuclear targets. These events were selected by requiring a negatively charged muon as well as a second track originating from the start of the muon track that has an energy deposition consistent with a pion and the presence of a Michel electron from the pion-muon-electron decay chain. The statistics shown are for 0.9×10^{20} POT, but a factor of 13 in statistics will be included in the published result.

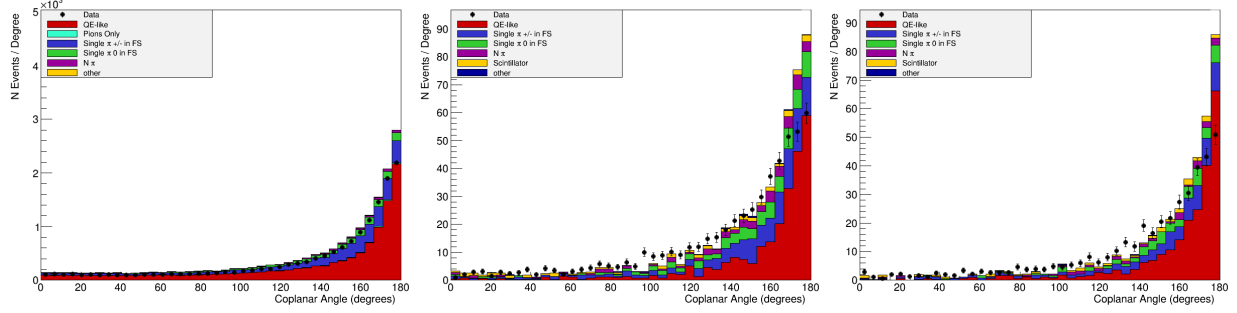


Figure 7: The angle between the neutrino-muon plane and the neutrino-proton plane in charged current quasielastic candidates in the Medium Energy beam, along with the prediction from GENIE. The plots show this angle for CH (left), and for two of our nuclear targets that are comprised of lead and iron (center and right). The signal process is in red and the *a priori* background predictions are in the other colors

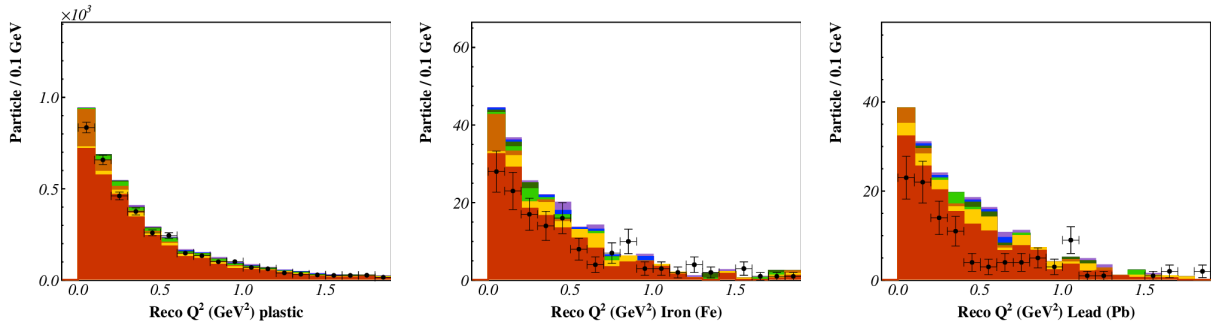


Figure 8: The square of momentum transferred to the nucleus in pion production candidates, for CH (left), iron (center) and lead (right). The signal process is in red and the other colors are the *a priori* background predictions.

2.4 Antineutrino Analysis Progress

MINERvA took 0.5×10^{20} POT in the last month of the FY16 accelerator run, which was 8 months before the next antineutrino-mode running began. These data have been calibrated and analyzed and investigations have begun addressing whether the analysis techniques developed in the low energy beam are still viable. Although the instantaneous event rates in these data are significantly higher, the first indications are that the analysis techniques deployed in the low energy beam are still effective. This section describes this early antineutrino data set, and makes projections for the statistics we expect for 12×10^{20} POT.

2.4.1 Charged Current Quasielastic Scattering in CH

For analyses of charged-current quasielastic scattering, the Medium Energy beam provides increased reach at high momentum transfer for measurements in CH. This is where the cross-section uncertainty is highest [6]. The sample shown in Figure 9 corresponds to 0.5×10^{20} POT, and contains 447 events that have momentum transfers between 2 and 4 GeV^2 . This means that MINERvA collects about a factor of four more events per proton on target in

the Medium Energy beam compared to the Low Energy beam, and will be able to map out the high momentum transfer region with 10,000 events in the 2-4 GeV² region of momentum transfer squared with 12×10^{20} POT.

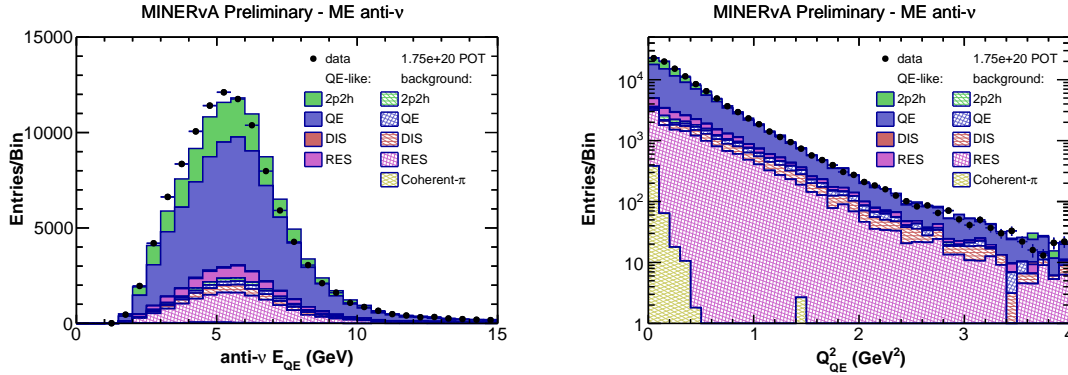


Figure 9: Neutrino energy (left) and momentum transfer (right) for the antineutrino charged current quasielastic sample, calculated assuming a quasielastic hypothesis.

2.4.2 Charged Current Quasielastic Scattering on Heavy Nuclei

The nuclear targets will provide thousands of charged current quasielastic (CCQE) events for an exposure of 12×10^{20} POT in antineutrinos. Figure 10 shows the event distributions along the vertical, horizontal and longitudinal axes of the detector for one-track events that pass CCQE cuts that begin either one plane before or two planes after the third nuclear target, which contains graphite, lead, and iron. Note that the scintillator background shown in the x and y distributions can be reduced by about a factor of three with tighter cuts on the vertex longitudinal position. These plots represent the statistics for 0.35×10^{20} POT, or a factor of 34 below our request.

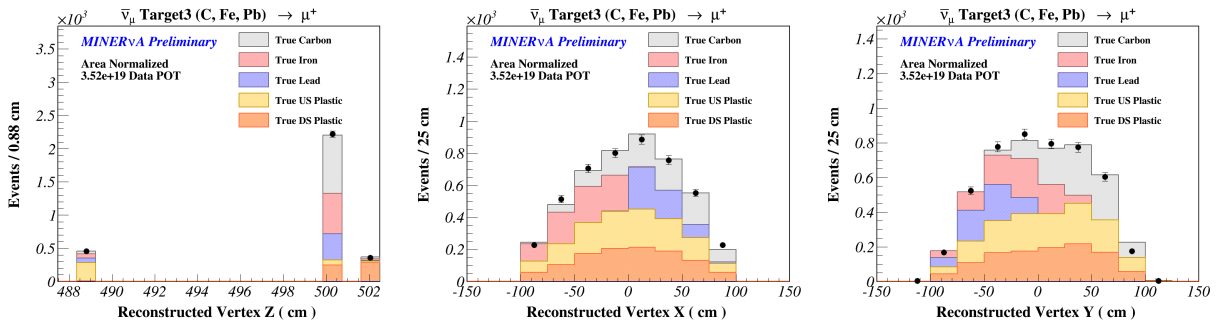


Figure 10: Longitudinal (z), horizontal (x) and vertical (y) event vertex distributions for CCQE candidates that start near nuclear target 3, for the data and the simulation.

2.4.3 Neutron Studies in the Medium Energy Antineutrino Beam

MINERvA's granularity and hydrocarbon target mean that neutrons that exit a neutrino-nucleus interaction can sometimes be measured in the detector through a small deposit of

energy. These deposits are only a small fraction of the neutron’s total energy, but they can provide information on the direction that a neutron was emitted from a neutrino-nucleon interaction. The angle between the neutron-neutrino plane and the muon-neutrino plane (the “coplanar angle”, or θ_c) in an antineutrino charged current quasielastic interaction, for example, can give some information about the role the nucleus plays there. This angle as measured for antineutrino interactions in the scintillator is shown in Figure 11. The sample size results from the first 0.4×10^{20} POT that MINERvA took in antineutrino mode on our 6 ton fiducial mass, and is about twice the sample size expected in the lowest mass (carbon) nuclear target given a 12×10^{20} POT exposure. In the iron and lead nuclear targets, we expect sample sizes a factor of 2-3 larger than that shown in Figure 11 with a 12×10^{20} POT exposure.

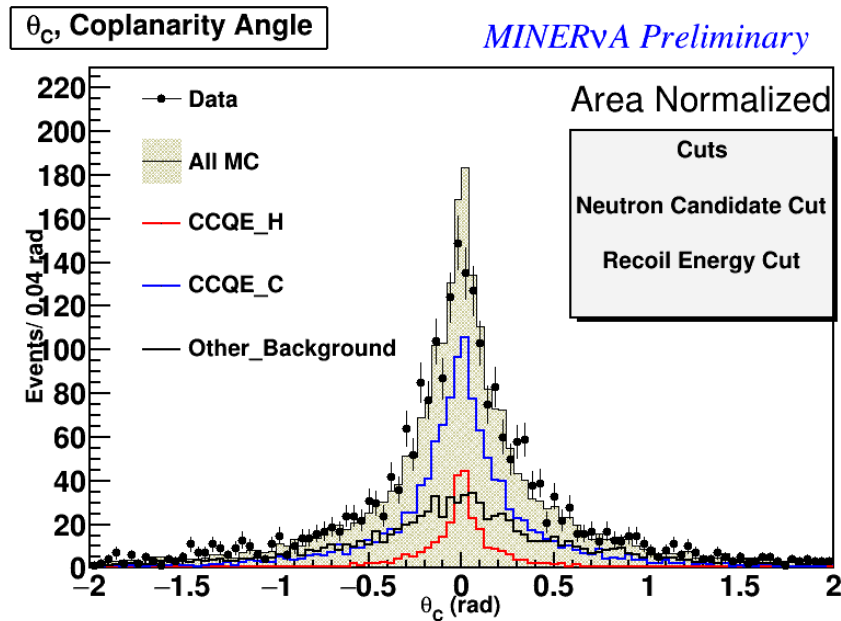


Figure 11: Distribution of the angle between the neutron-neutrino plane and the muon-neutrino plane for quasielastic-like events in the first 0.4×10^{20} POT of antineutrino running that MINERvA took. The narrow peak predicted from interactions off hydrogen is shown in addition to the broader peak predicted from interactions with carbon.

2.4.4 Pion Production and Deep Inelastic Scattering

The Medium Energy beam will also provide high statistics samples of events with final state pions, which will dominate event rates at DUNE. MINERvA’s low energy analyses indicate these pions are strongly impacted by nuclear effects such as final state interactions, and that these effects modify neutrino and antineutrino channels differently. Increased statistics in the Medium Energy beam, particularly in the case of antineutrinos, will provide needed detail for understanding which effects are important. The MINERvA detector is particularly well suited for studying coherent pion production [7], and we have made precise measurements of this process in the low energy beam for both neutrinos and antineutrinos. A 12×10^{20} POT

exposure in antineutrino mode will provide a few thousand events in the nuclear targets, making feasible studies of antineutrino coherent pion production as a function of atomic number.

Deep Inelastic Scattering (DIS) will also be an abundant source of events at DUNE. Our original justification for a 12×10^{20} POT exposure focused on our plan to measure the EMC effect in antineutrino-mode DIS events to the few percent level in several Bjorken x bins. Figure 12 shows projected statistical uncertainties on $\nu/\bar{\nu}$ DIS cross-section ratios as a function of Bjorken- x for carbon and lead. The statistical uncertainty for the iron ratio will be similar to that of lead. Also shown in Figure 12 are predicted ratios from a model by Cloet, which predicts the ratio between neutrino and antineutrino modes to differ significantly as x increases.

Since 2015, interest in nuclear effects in antineutrino DIS has grown beyond just the region defined by the ‘‘EMC effect’’. Several nuclear parton distribution studies of neutrino-Fe [8][9] and a direct experimental comparison of electron-Fe with neutrino-Fe structure functions [10] have demonstrated a surprising difference in the low Bjorken- x shadowing region. The high statistics and expanded kinematic range enabled with the Medium Energy beam offers a unique ability to also examine these Bjorken- x dependent nuclear effects with antineutrinos from the low x shadowing region up through the higher x EMC effect region.

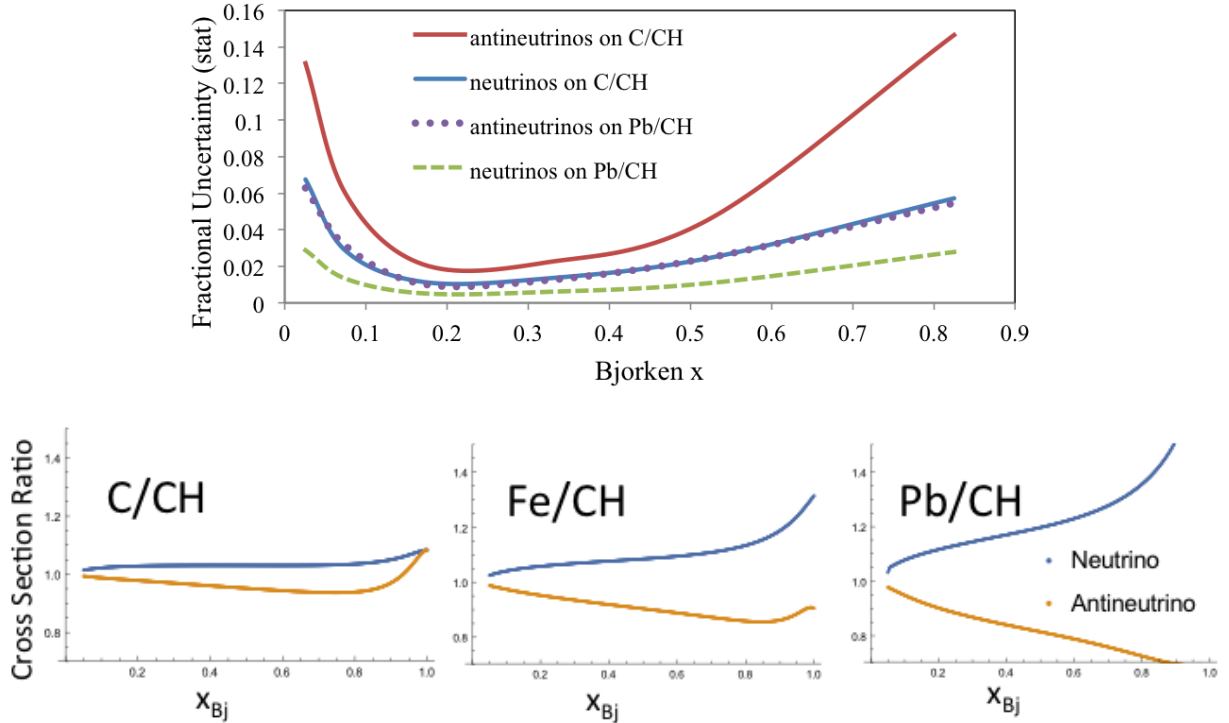


Figure 12: Top: Fractional uncertainties on neutrino and antineutrino DIS cross-section ratios to scintillator for carbon and lead as a function of x_{Bj} bin, for an exposure of $(12 \times 10^{20}$ POT) in neutrinos (antineutrinos). These are to be compared to the lower plots which show the predicted ratios in a model by Cloet [11][12]

Target Material	fiducial mass (kg)	1-track CCQE	neutron-tagged CCQE	high Q^2 CCQE	CC coherent pions	DIS (all targets)
C	160	30,000	2,000	260	600	3,000
Pb	729	140,000	9,000	1,200	2,500	18,000
Fe	641	120,000	8,000	1,000	2,200	18,000
Water	452	90,000	5,500	750	1,500	8,000
CH	6000	1,100,000	70,000	10,000	21,000	110,000

Table 1: Expected event statistics for 12×10^{20} POT in antineutrino mode, as a function of interaction channel and target nucleus. For the DIS analysis all targets are used, but for the remaining analyses only the downstream four targets are used. For the water target, the entries are for the scenario that there is no empty target running.

2.5 Summary of Impact of 12×10^{20} POT of Antineutrino Data

Table 2.5 summarizes the statistics for a few key analyses for a 12×10^{20} exposure. We note that essentially all antineutrino analyses will benefit from such an exposure, which would enable many multi-dimensional cross-section measurements. The cross sections on carbon play a special role: for some analyses they serve as a cross check that the experiment is modeling detector acceptance in the nuclear targets well because the ratio between carbon and the CH of the plastic is expected to be very close to one. For other analyses the comparison between C and CH could give rise to a measurement of scattering off hydrogen.

There are many other analyses, not discussed here for the sake of brevity, that would be compelling with a 12×10^{20} POT antineutrino exposure. For example electron neutrino CCQE measurements could be measured on CH over a broad range of momentum transfers. In addition, even at 12×10^{20} POT the antineutrino electron scattering absolute flux constraint is likely to be statistics dominated. The ν_e CCQE measurement would be utilized by NOvA, T2K, and DUNE, and the absolute flux constraint could be used by any experiment using the NuMI beamline.

3 Low Energy Results and Impact to Oscillation Experiments

Publication of Low Energy data began in 2013, and the collaboration has now published 20 papers using those data, half of which are in Physical Review Letters. This far surpasses the number of cross-section publications by any modern neutrino experiment (see Table 2). These papers describe measurements of a wide variety of processes, including pion and kaon production, quasielastic, diffractive, elastic and deep inelastic scattering, as well as inclusive cross sections. Approximately seven Low Energy analyses are ongoing, with most in paper-writing or paper-review stages.

Because of the limited sample size, the low-energy measurements have focused on cross sections using the MINERvA tracker, which is primarily scintillator (CH). For processes with higher sample sizes, measurements of double-differential cross sections are possible in this dataset, and have proven very valuable to the model-tuning and oscillation communities.

Table 2: Summary of cross-section publications by modern accelerator-based neutrino experiments.

Published σ Papers	PRL	PRD	PLB	Total
MINERvA	10	9	1	20
T2K	2	12		14
MiniBooNE	2	8		10
ArgoNeuT	2	3		5
SciBooNE		5		5
MINOS		3		3
NOvA				0
MicroBooNE				0

An example of such an analysis comes from the charged-current inclusive sample shown in Figure 13. This analysis reconstructs variables similar to those commonly used in electron-scattering experiments, which enables separation of processes such as quasielastic scattering, multi-nucleon (2p2h) interactions, and pion production.

The inclusive data in Figure 13 show a deficit in GENIE models at moderate hadronic energies even after inclusion of the latest 2p-2h models that partially fill in this region. The MINERvA collaboration has performed a fit to these data, and finds that the best fits are obtained when the GENIE 2p-2h contribution is enhanced by approximately 60%. This tuned model also provides better agreement in other analyses, such as neutrino quasielastic scattering (see Figure 14). This tuned model was requested by and provided to the T2K, NOvA, DUNE and MicroBooNE collaborations, who are currently working to understand the impact of this model on their oscillation analyses.

We are in the process of finalizing an analysis that uses this same technique in the Low Energy antineutrino beam, and we will be extending this suite of measurements to the nuclear target regime for both neutrino and antineutrino modes in the Medium Energy beam.

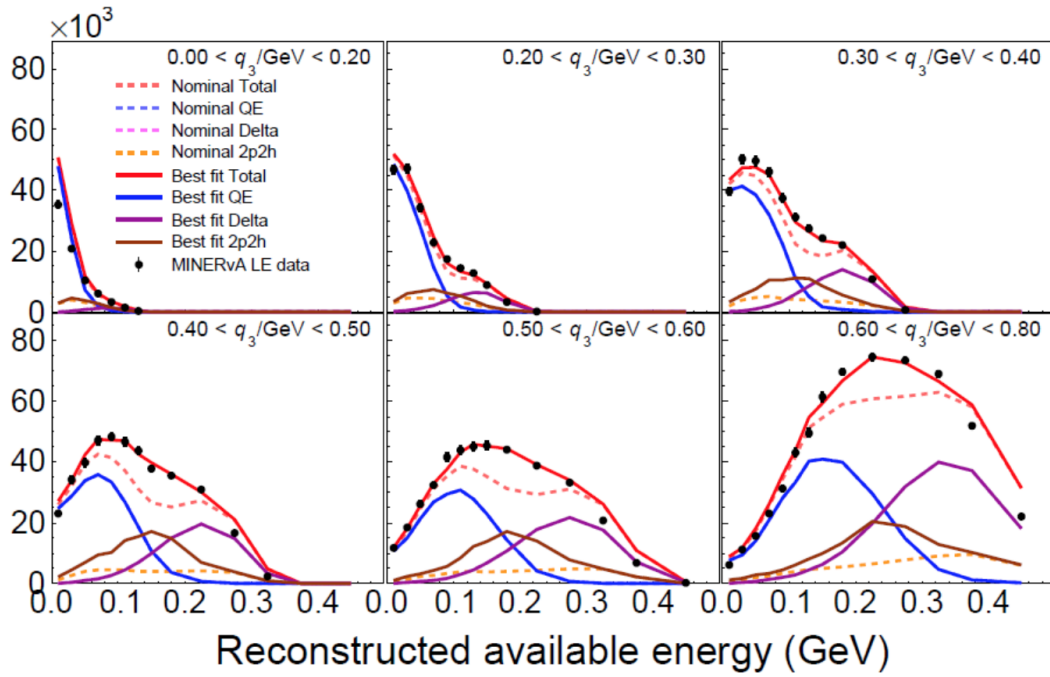


Figure 13: Inclusive charged current cross event rates as a function of hadronic recoil energy in bins of reconstructed 3-momentum transfer (q_3) in MINERvA data (black points). The solid lines show GENIE predictions for various subprocesses and the total (red), while the dotted lines show those same models tuned to the MINERvA data.

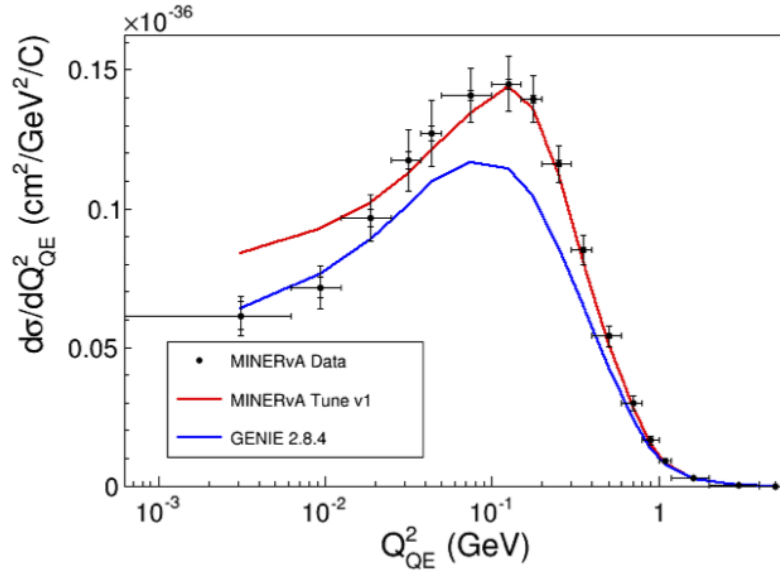


Figure 14: Reconstructed four-momentum transfer squared reconstructed assuming a quasielastic hypothesis in the MINERvA low energy 0-pi analysis (data points), compared with GENIE models before and after tuning to MINERvA inclusive data shown in Figure 13.

4 Detector Performance and Cost of Operations

The MINERvA collaboration strives to minimize downtimes due to detector maintenance and has achieved livetimes of greater than 96% for the MINERvA detector and 91% for MINERvA combined with the MINOS near detector, which serves as MINERvA’s muon spectrometer. POT, both delivered to the experiment and recorded, are summarized in Figure 15.

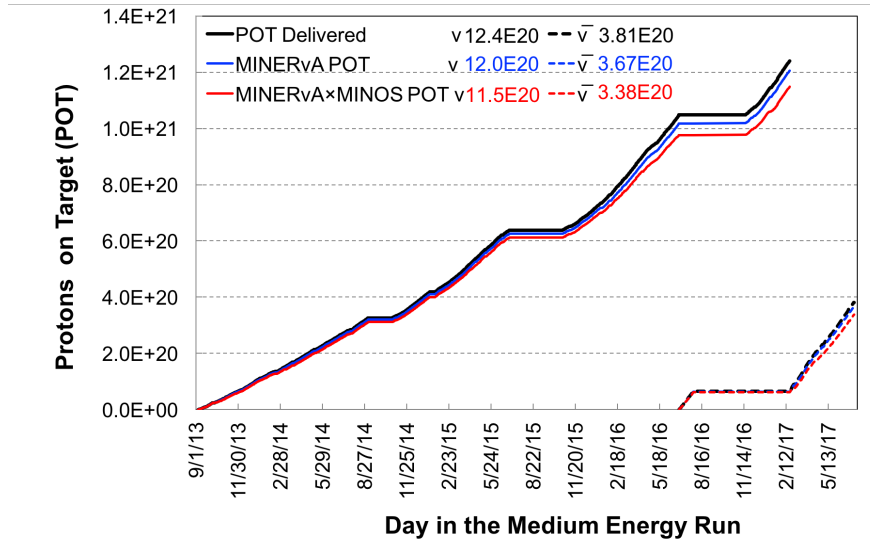


Figure 15: POT delivered to MINERvA (black), while the MINERvA detector was live (blue), and while the MINERvA and MINOS detectors were live (red). The solid (dashed) lines show POT delivered while NuMI was in a neutrino (antineutrino) mode configuration.

MINERvA data are calibrated to account for a number of effects such as photomultiplier gains and scintillator light levels that change over time [13]. The calibrated number of photoelectrons associated with minimum-ionizing muons is shown in Figure 16. While light levels have fallen over the lifetime of the experiment, they are still quite strong. Based on measurements done in MINERvA’s prototyping stage and given the current rate of light yield loss, MINERvA’s position resolution by March 2023 will have degraded by about 30% compared to its initial light levels [14]. By 2023, MINERvA would have far surpassed 12×10^{20} POT in integrated antineutrino running.

4.1 NuMI Beam Monitoring

At the end of June 2016, the MINOS collaboration stopped taking data with the MINOS Far Detector and stopped contributing to Near Detector operations. The MINERvA collaboration is now responsible for detector operations, calibrations, and data processing, and has taken over routine maintenance of the MINOS electronics. As part of this work, the collaboration monitors neutrino energy spectra in the MINOS near detector over time in order to verify the stability of the NuMI beam. Figure 17 shows the neutrino energy spectrum in the Near Detector for several intervals during recent antineutrino running. Two regions, in

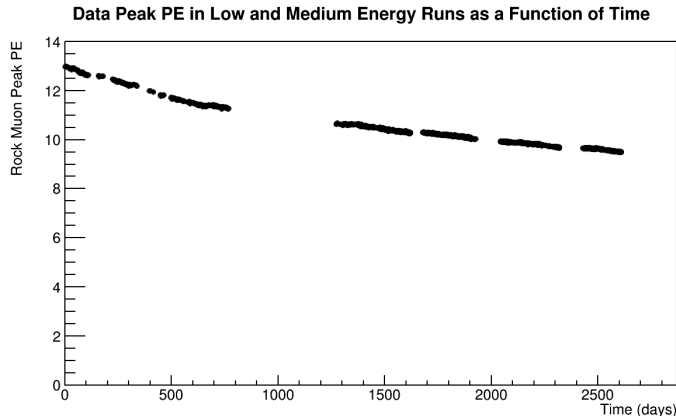


Figure 16: Average number of photo-electrons per MINERvA strip produced by through-going muons, from the start of MINERvA data taking through May 2017.

June and July of 2016, show deviations from the average and are due to a tilt of the first NuMI horn outside of tolerance. Since that tilt was corrected, the energy spectrum has been extremely stable. NOvA is not able to monitor the beam in this manner, since at NOvA’s off-axis detector angle, pions from many energies contribute neutrinos at the same energy. In the on-axis detectors, the beamline can be monitored because different beamline problems will change the measured neutrino energy spectrum in different ways.

4.2 Operations cost

The incremental cost of operating the MINERvA and MINOS detectors is modest once the NuMI beamline is operating for the NOvA experiment. Fiscal year 2017 is an appropriate year for extrapolations to the next years because we did not purchase any additional helium to fill the cryogenic target and did not purchase significant spare stock in any electronics components. In FY2017 Fermilab spent \$115k on MINERvA and MINOS together in Materials and Services. This was dominated by yearly costs to repair MINOS electronics and purchase software licenses. In addition, a total of 2230 hours were charged to MINERvA operations, or 1.24 FTE worth of effort spread over many people.

The MINERvA collaboration has streamlined its operations procedures at no loss of data-taking efficiency and now runs checklist-based shifts which require an active shift taker for only 8 hours throughout a 24-hour period. The collaboration itself dedicates 4.6 FTE towards Detector operations (or about 10% of the full FTE of the collaboration), including the 1 FTE of shift taking [15].

The collaboration also dedicates 2.6 FTE (6% of the collaboration) towards computing operations [15]: this includes keepup processing for both the MINERvA and MINOS detectors, production and software releases. The keepup processing which is the only thing that is dependent on operations is 0.5 FTE.

Fermilab’s Scientific Computing Division (SCD) expends about \$42k per year on media, and \$136k per year on the roughly 16 million CPU hours that are used each year to process MINERvA jobs. These costs are dominated by the size of the existing Medium Energy

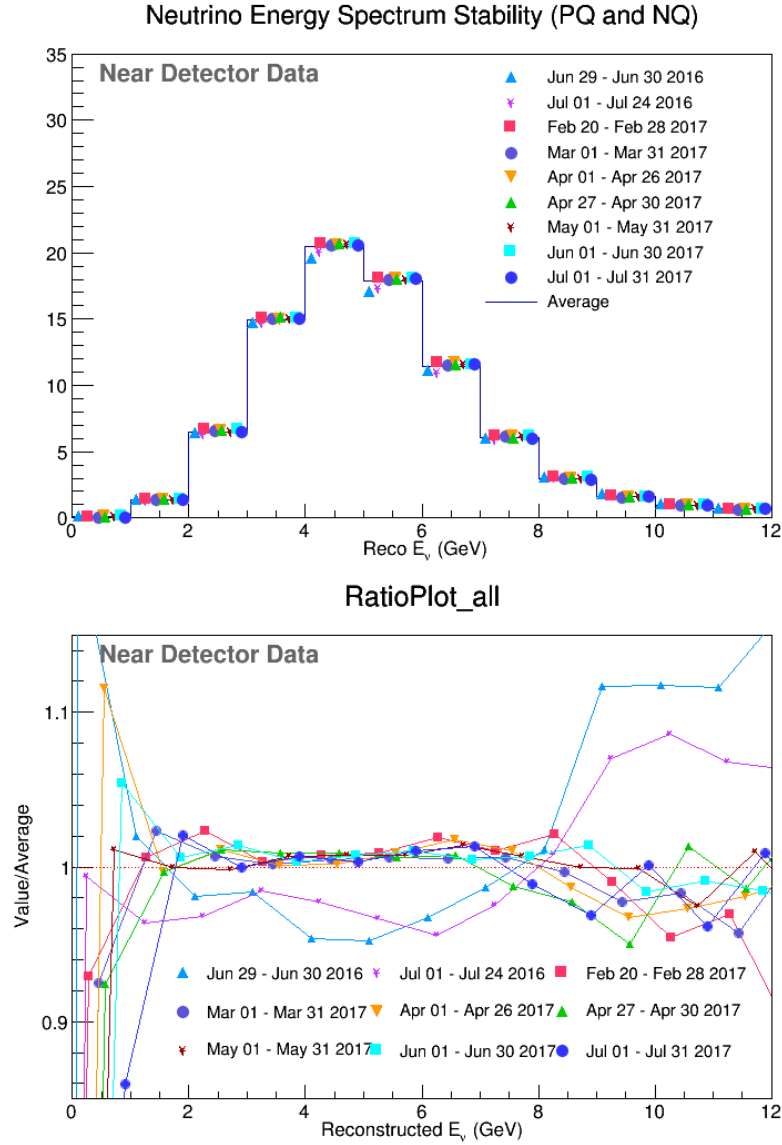


Figure 17: Antineutrino energy spectra in the MINOS near detector for several periods of running (above), and ratios of each of these spectra to the average (below). The two run periods that are different from the others correspond to a time when the most upstream horn was tilted with respect to nominal by 1.4mrad.

dataset, and the incremental computing cost of taking 12×10^{20} POT over 6×10^{20} POT in antineutrino mode will be minimal. Similarly, SCD provides personnel to help with software development, computing operations, and computing facilities. These personnel work on many intensity frontier experiments and the incremental labor associated with MINERvA is 1.72 FTE [16].

References

- [1] MINERvA's Medium Energy Program, Report submitted to the January 2015 Fermilab Physics Advisory Committee, <http://minerva-docdb.fnal.gov/cgi-bin/ShowDocument?docid=10568>
- [2] J. Park *et al.* [MINERvA Collaboration], Phys. Rev. D **93**, no. 11, 112007 (2016) doi:10.1103/PhysRevD.93.112007 [arXiv:1512.07699 [physics.ins-det]].
- [3] A. Bodek, U. Sarica, D. Naples and L. Ren, Eur. Phys. J. C **72**, 1973 (2012) doi:10.1140/epjc/s10052-012-1973-6 [arXiv:1201.3025 [hep-ex]].
- [4] L. Ren *et al.* [MINERvA Collaboration], Phys. Rev. D **95**, no. 7, 072009 (2017) doi:10.1103/PhysRevD.95.072009 [arXiv:1701.04857 [hep-ex]].
- [5] L. Aliaga *et al.* [MINERvA Collaboration], Phys. Rev. D **94**, no. 9, 092005 (2016) Addendum: [Phys. Rev. D **95**, no. 3, 039903 (2017)] doi:10.1103/PhysRevD.94.092005, 10.1103/PhysRevD.95.039903 [arXiv:1607.00704 [hep-ex]].
- [6] A. S. Meyer, M. Betancourt, R. Gran and R. J. Hill, Phys. Rev. D **93**, no. 11, 113015 (2016) doi:10.1103/PhysRevD.93.113015 [arXiv:1603.03048 [hep-ph]].
- [7] A. Higuera *et al.* [MINERvA Collaboration], Phys. Rev. Lett. **113**, no. 26, 261802 (2014) doi:10.1103/PhysRevLett.113.261802 [arXiv:1409.3835 [hep-ex]].
- [8] K. Kovarik, I. Schienbein, F. I. Olness, J. Y. Yu, C. Keppel, J. G. Morfin, J. F. Owens and T. Stavreva, Phys. Rev. Lett. **106**, 122301 (2011) doi:10.1103/PhysRevLett.106.122301 [arXiv:1012.0286 [hep-ph]].
- [9] S. X. Nakamura *et al.*, Rept. Prog. Phys. **80**, no. 5, 056301 (2017) doi:10.1088/1361-6633/aa5e6c [arXiv:1610.01464 [nucl-th]].
- [10] N. Kalantarians, C. Keppel and M. E. Christy, Phys. Rev. C **96**, no. 3, 032201 (2017) doi:10.1103/PhysRevC.96.032201 [arXiv:1706.02002 [hep-ph]].
- [11] I. C. Cloet, W. Bentz and A. W. Thomas, Phys. Rev. Lett. **109**, 182301 (2012) [arXiv:1202.6401 [nucl-th]].
- [12] I. C. Cloet, private communication
- [13] L. Aliaga *et al.* (MINERvA Collaboration), Nucl. Instrum. Meth. **A743** 130-159, (2014).

- [14] J. Chvojka, MINERvA-docdb 1592, (2007).
- [15] D. Harris and K. McFarland, Resource Usage talk at MINERvA Operations Review of October 2016, MINERvA-docdb 12594 (2016).
- [16] MINERvA Experimental Operations Plan, v4.4, February 24, 2017.